Molecular & Cellular Biomechanics

Tech Science Press

Intramyocardial Injections to De-Stiffen the Heart: A Subject-Specific in Silico Approach

Yaghoub Dabiri[1,3], Kevin L. Sack[1,2], Semion Shaul[1], Gabriel Acevedo-Bolton[1], Jenny S. Choy[3], Ghassan S. Kassab[3] and Julius M. Guccione[1,*]

[1]Department of Surgery, University of California San Francisco, San Francisco, California, USA.

[2]Division of Biomedical Engineering, Department of Human Biology, University of Cape Town, Cape Town, South Africa.

[3]California Medical Innovations Institute, San Diego, California, USA.

[*]Corresponding Author: Julius M. Guccione. Email: Julius.Guccione@ucsf.edu.

Abstract: We hypothesized that minimally invasive injections of a softening agent at strategic locations in stiff myocardium could de-stiffen the left ventricle (LV) globally. Physics-based finite element models of the LV were created from LV echocardiography images and pressures recorded during experiments in four swine. Results confirmed animal models of LV softening by systemic agents. Regional de-stiffening of myocardium led to global de-stiffening of LV. The mathematical set up was used to design LV global de-stiffening by regional softening of myocardium. At an end diastolic pressure of 23 mmHg, when 8 ml of the free wall was covered by intramyocardial injections, end diastolic volume (EDV) increased by 15.0%, whereas an increase up to 11 ml due to intramyocardial injections in the septum and free wall led to a 26.0% increase in EDV. Although the endocardial intramyocardial injections occupied a lower LV wall volume, they led to an EDV (44 ml) that was equal compared to intramyocardial injections in the mid-wall (44 ml) and larger compared to intramyocardial injections in the epicardium (41 ml). Using an in silico set up, sites of regional myocardium de-stiffening could be planned in order to globally soften overly stiff LV in heart failure with preserved ejection fraction. This novel treatment is built on subject-specific data. Hypothesis-testing of these simulation findings in animal models is warranted.

Keywords: HFpEF; injection treatment; myocardium; subject-specific; finite element modeling

1 Introduction

Approximately 50% of patients with heart failure (HF) have preserved ejection fraction [7,24], a life-threatening disease for which optimal treatments remain controversial [5,31]. Moreover, the population of patients with HF with preserved ejection fraction (HFpEF) has increased in the past, and will continue to increase [4,14,22]. HFpEF can cause end-stage HF, for which the extremely limited treatment options are mechanical circulatory support devices or heart transplantation. These treatment options, if available, are risky and expensive.

Experimental and computational studies have shown that intramyocardial injection treatment can be beneficial for patients with HF [18,19,23,32,33]. We hypothesized that minimally invasive intramyocardial injections of ALT-711 (phenyl-4,5-dimethylthazolium chloride) at strategic locations in the stiff myocardium (that has an abnormally stiff extracellular matrix (ECM)) could be used to soften LV globally. The efficacy and safety of this agent in de-stiffening overly stiff LV has been reported in the literature 1,20,21]. Minimally invasive intramyocardial injection of ALT-711 may be an effective treatment for HFpEF, which is linked to overly stiff myocardium. We have known since 1991 [13] that the mechanical properties of the ECM in the normal LV are non-linear and anisotropic (i.e., transversely isotropic with respect to the local muscle fiber or

myofiber direction). In other words, the stiffness of the ECM increases as it is stretched, and the ECM is approximately three times stiffer in the myofiber direction than in a plane perpendicular or transverse to the myofiber direction [13], even when the heart muscle or myocardium is not contracting. Here, we used cardiac catheterization Real-time 3D transesophageal echocardiography (RT3D-TEE) and finite element (FE) modeling to quantify the mechanical properties of myocardium before and after aortic banding. We then used physics-based left ventricle (LV) FE models to simulate regional myocardium "de-stiffening" to increase LV end diastolic volume (EDV). The primary reason for using intramyocardial injections for HFpEF is to halt decreased EDV caused by extracellular pathways in HFpEF [6,27].

2 Methods

2.1 Animal Experiments

All animal experiments were performed in accordance with national and local ethical guidelines, including the Guide for the Care and Use of Laboratory Animals, the Public Health Service Policy on Humane Care and Use of Laboratory Animals, and the Animal Welfare Act, and an approved California Medical Innovations Institute IACUC protocol regarding the use of animals in research.

In vivo data were obtained from swine studies in which the geometry and pressure data were obtained (Tab. 1). For each animal (n = 4), end diastolic pressure volume relationship (EDPVR) was measured at multiple time points after aortic banding. For this study, data points with high LV stiffness were used. A hockey-stick guiding catheter was advanced over a wire through the introducer sheath towards the LV to measure pressure, and the EDV was obtained from RT3D-TEE images. Then these two findings were used to approximate EDPVR as described by Klotz and colleagues [17]. The echocardiography images and LV pressure at the base-line state, and several weeks after aortic banding were used for computational modeling as described in Section 2.2.

Table 1: EDV and EDP for four pigs used in the study

	Baseline		Overly stiff LV	
	EDV	EDP	EDV	EDP
Pig ID				
1	49.3	11.4	50.9	18.3
2	68.3	4.4	86.1	19.6
3	69.5	16.0	54.7	24.2
4	41.9	13.5	40.0	23.2

2.2 Computational Modeling

The computational modeling was performed using the data for all animals (Tab. 1). Remodeling of LV due to supra-valvular aortic banding was quantified using RT3D-TEE. The LV geometry during early diastolic filling was reconstructed from the RT3D-TEE images [8], and then the geometry was meshed using TrueGrid (XYZ Scientific Applications Inc, Pleasant Hill, California, USA). To further illustrate, a sample echo image, reconstructed geometries and a sample mesh are shown in Figs. 1(a)-1(d).

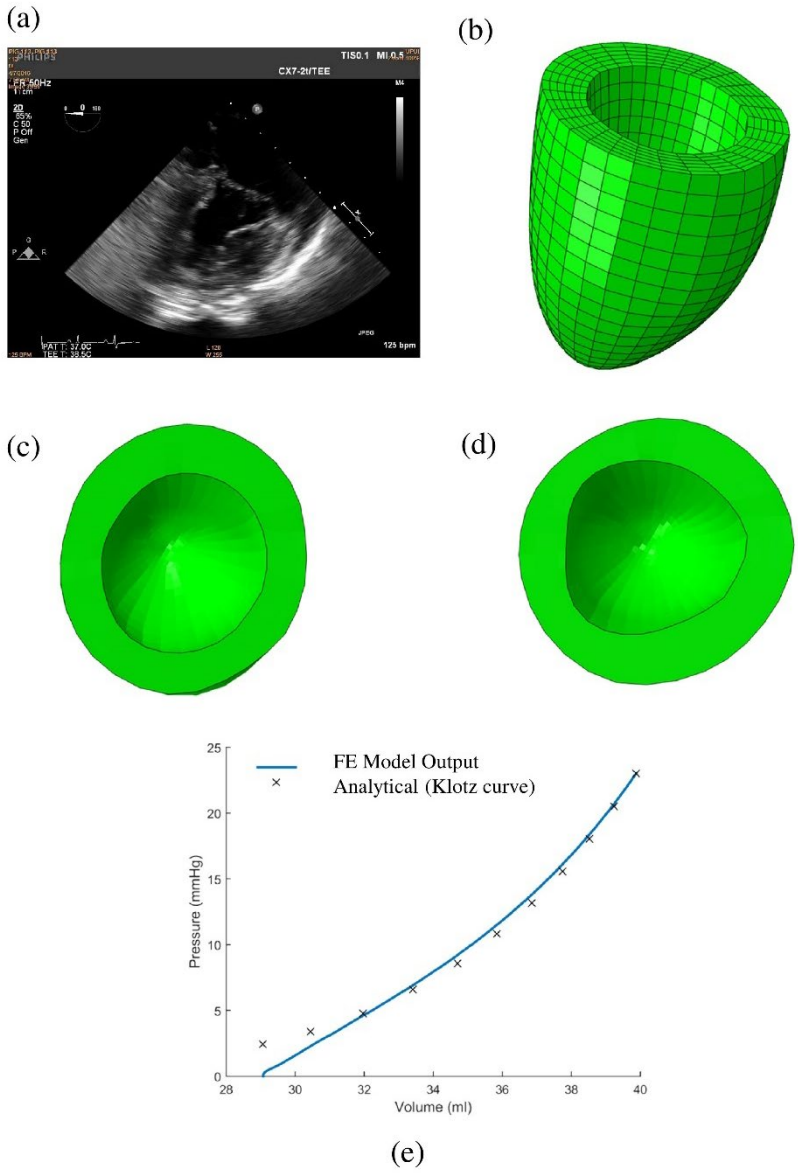

Figure 1: Geometry reconstruction and material calibration. (a) The echocardiography images were obtained from swine. Philips Dicom Viewer software (Philips Medical Systems, Best, Netherlands) was used to show the example end systolic echo images. (b) TrueGrid was used to mesh the reconstructed geometry. The short-axis views of the LV at (c) baseline and (d) 6 weeks after aortic banding. (e) The material parameters were determined using the analytical curve suggested by Klotz and colleagues [17]

ABAQUS software was used for FE computations (Simulia, Providence, RI, USA). The main structure of the model follows the one described in the Living Heart Project literature [3].

The constitutive equations for the material behavior are based on the fiber-reinforced model described in the literature [11,16]. The following strain energy function is used to calculate passive tissue stress:

$$\Psi_{dev} = \frac{a}{2b} e^{b(I_1-3)} + \sum_{i=f,s} \frac{a_i}{2b_i} \left\{ e^{b_i (I_{4i}-1)^2} - 1 \right\} + \frac{a_{fs}}{2b_{fs}} \left\{ e^{b_{fs} (I_{8fs})^2} - 1 \right\} \quad (1)$$

$$\Psi_{vol} = \frac{1}{D}\left(\frac{J^2-1}{2} - \ln(J)\right) \quad (2)$$

Here, a and b are isotropic stiffness material parameters of the tissue. The parameters with subscripts f, s, and fs refer to material parameters associated with additional stiffness in the myofiber direction, sheet direction, and the connection between myofiber and sheet directions. The invariants, I_1 , I_{4i} and I_{8fs} are:

$$I_1 := \mathrm{tr}(\mathbf{C})$$
$$I_{4i} := \mathbf{C} : (\mathbf{i}_0 \otimes \mathbf{i}_0)$$
$$I_{8fs} := \mathbf{C} : \mathrm{sym}(\mathbf{f}_0 \otimes \mathbf{s}_0) \quad (3)$$

Here, $\mathbf{C}$, $\mathbf{f}_0$ and $\mathbf{s}_0$ are the right Cauchy-Green tensor, and vectors for the local myofiber and sheet directions, respectively. J is the determinant of the deformation gradient, and $D = 2/K$ with K being the Bulk modulus. The myofiber angles were assumed to change from -60º in the epicardium to 60º in the endocardium [10,29]. The total stress in the LV tissue was the sum of passive and active stress. The active stress was computed using the formula reported by Guccione and colleagues [12]. The relevant mechanical properties are summarized in Tab. 3.

To account for the effects of intramyocardial injections on the passive material properties, the material definition was adjusted as follows [26]:

$$\Psi_{dev} = \frac{\bar{a}}{2b} e^{b(I_1-3)} + \sum_{i=f,s} \frac{\bar{a}_i}{2b_i}\left\{e^{b_i(I_{4i}-1)^2} - 1\right\} + \frac{\bar{a}_{fs}}{2b_{fs}}\left\{e^{b_{fs}(I_{8fs})^2} - 1\right\} \quad (4)$$

with

$$\bar{a} = a\left[P_{scaling}C_{index} + (1 - C_{index})\right] \quad (5)$$

where, C_{index} is a regionally varying description of ALT-711 injection concentration, and $P_{scaling}$ is a constant that scales the passive response linearly with respect to C_{index}. The regional influence of the ALT-711 injection is at a maximum with $C_{index} = 1$ and has no effect with $C_{index} = 0$. For regions within 5 mm from injection center Cindex=1 and for regions within 5 to 10 mm from injection regions, Cindex changed linearly with distance from injection center. To model the intramyocardial injections, we did not alter the geometry of the myocardium but only changed the material properties. The alterations caused by injections represent effective properties of myocardium and injections together. We assumed injections do not add volume to LV wall volume, and only affect the tissue behavior (temporary injection volumes were not considered). The injection is a substance that will change the passive or diastolic mechanical properties of the myocardium in the vicinity of the injection site. Unlike our previous studies where a non-contractile material was used for treatment of heart failure with reduced ejection fraction, the injectate in this study is not intended to support any load [8,19,33].

To determine subject-specific material constants we uniformly scaled the constants in Eq. (1) by two parameters A (for a, a_f, a_s, a_{fs}) and B (for b, b_f, b_s, b_{fs}), which were determined according to the analytical volume-pressure curves reported by Klotz and colleagues [9,17,26] (Fig. 1(e)).

One of the models with high LV stiffness was used to assess the effects of injection properties (pig #4, 6 weeks after aortic banding, Tab. 1). A range of 1-16 intramyocardial injections was made in the LV free wall (Fig. 2). To examine the effects of intramyocardial injections in the septum, an additional 12 intramyocardial injections were made in the septum. Two shapes of intramyocardial injections, cylindrical and spherical, were simulated. Cylindrical intramyocardial injections extended from the endocardium to the epicardium regions, whereas spherical intramyocardial injections were centered at each injection site. To examine the effects of injection stiffness, EDV was calculated for the 1-16 spherical intramyocardial injections with $P_{scaling}$ altered at 0.01, 0.3, 0.5, 0.7, and 0.9.

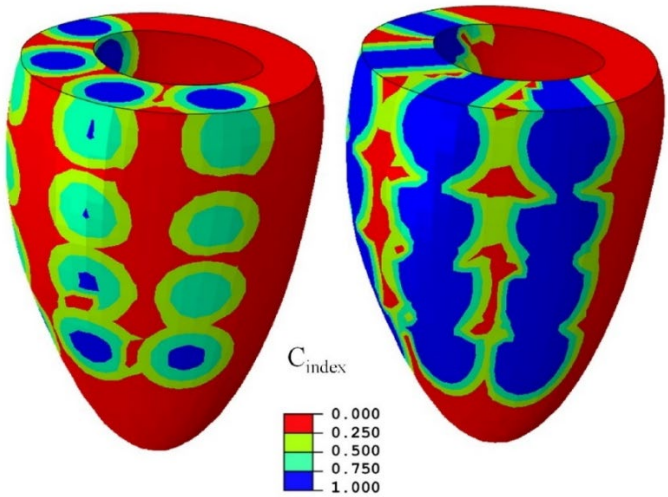

Figure 2: Site and shape of intramyocardial injections made in the LV free wall. The free wall injections were made in a 4 × 4 pattern. A set of 12 injections was also made in the septum. Two shapes of injections were used: spherical (left) and cylindrical (right). Three transmural locations for injections were used: epicardium, mid-wall and endocardium. This is a three dimensional view with the free wall on the left side

3 Results

The EDV increased as the volume of intramyocardial injections increased. Moreover, the stiffness of the injected region influenced EDV. When the stiffness decreased, the EDV increased (Fig. 3). The highest EDV (44 ml) was obtained with 16 intramyocardial injections (volume = 8 ml) and lowest stiffness scale ($P_{scaling} = 0.01$).

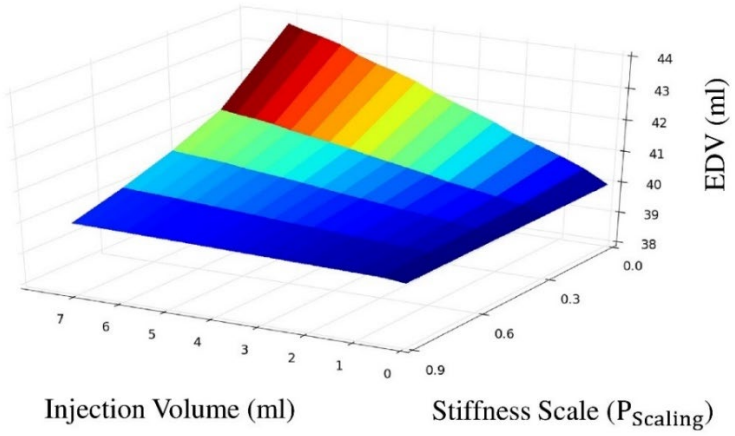

Figure 3: EDV *vs.* injection volume and stiffness. The EDV increased with the volume of intramyocardial injections. Mid-wall spherical intramyocardial injections were used for this surface

Intramyocardial injections perturbed end systolic strain. In the untreated case, the LV mainly experienced compressive strain in the myofiber direction. Unlike in the untreated case, tensile strains in the myofiber direction were seen at the sites of intramyocardial injections located proximal to the base and/or epicardium. Compared to the untreated case, compressive strains in the myofiber direction increased at the injection sites within the endocardium and close to the apex (Fig. 4).

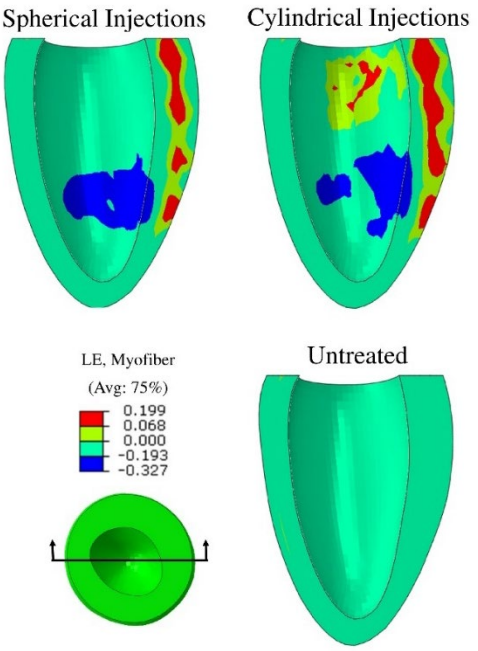

Figure 4: End-systolic logarithmic strain distribution in the myofiber direction. The end-systolic strains in the myofiber direction were altered by intramyocardial injections. The results pertain to 16 cylindrical and 16 mid-wall spherical intramyocardial injections ($P_{scaling}$ = 0.01). Injection volumes are summarized in Tab. 2. This is a long-axis view with the cut plane as shown

The EDPVR shifted toward higher EDVs when the intramyocardial injections were made in both septum and free wall, than when they were only within the free wall (Fig. 5). Both spherical and cylindrical intramyocardial injections led to higher EDV when made in the free wall and the septum, whereas cylindrical intramyocardial injections led to higher EDVs. At EDP = 23 mmHg, the cylindrical intramyocardial injections and spherical intramyocardial injections in the free wall and septum led to EDV = 50 and 47 ml, respectively (Tab. 2).

Table 2: The EDV for normal base-line, untreated pressure overload, and intramyocardial injection treated states for the pig #4. The injection volume represents the region where C_{index} = 1.0 (The dark blue region in Fig. 2)

Intramyocardial injection shape	Intramyocardial injection Volume (ml)	EDV (ml)
Healthy Base-line	NA	42
Untreated Pressure Overload*	NA	40
Spherical Intramyocardial injections		
Free wall		
Mid-wall	7	44
Endocardium	4	44
Epicardium	4	41
Free wall and septum	12	47
Cylindrical Intramyocardial injections		
Free wall	8	46
Free wall and septum	11	50

Table 3: The mechanical properties for four pigs

	Properties							
Pig ID	**a (MPa)**	**b**	**a_f (MPa)**	**b_f**	**a_s (MPa)**	**b_s**	**a_{fs} (MPa)**	**b_{fs}**
1	5.781e-3	12.356	1.906e-2	23.709	2.646e-3	20.558	1.555e-3	5.0595
2	1.338e-3	6.222	4.4080e-3	11.938	6.122e-4	10.351	3.540e-4	2.548
3	8.840e-4	31.303	2.914e-3	60.065	4.047e-4	52.081	2.377e-4	12.818
4	6.834e-3	11.917	2.253e-2	22.867	3.128e-3	19.828	1.838e-3	4.880

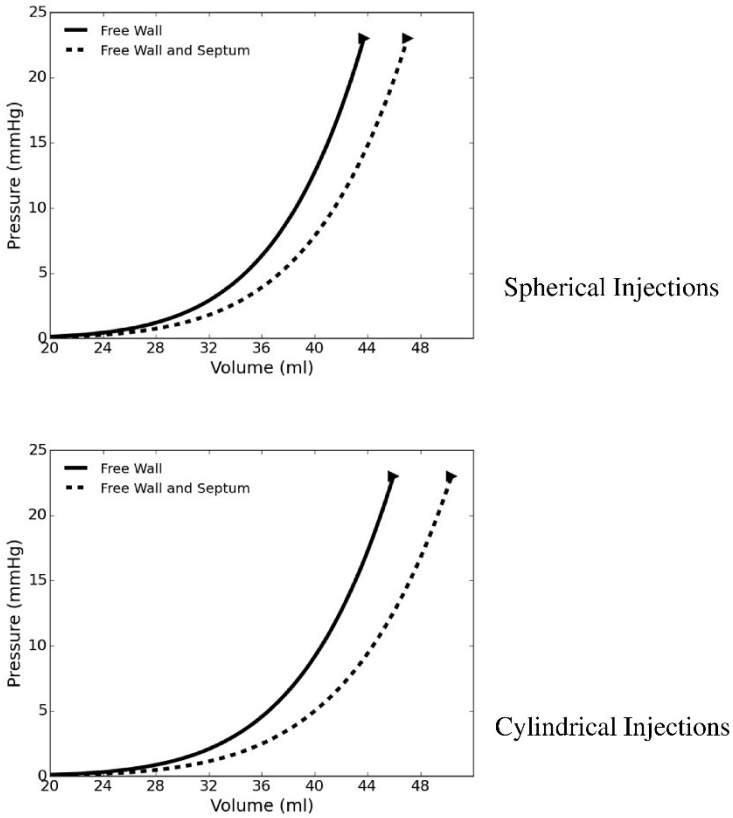

Figure 5: ED PVR for intramyocardial injections in the free wall with/without septum. Injections in the septum and free wall led to higher diastolic LV volumes at all diastolic LV pressures compared to injections only in the free wall with either mid-wall spherical or cylindrical injections. The triangle shows EDV, EDP

The intramyocardial injections in the free wall shifted the EDPVR toward higher EDVs compared to the untreated case (Fig. 6). The cylindrical intramyocardial injections had greater effects on increasing EDV compared to spherical intramyocardial injections. At EDP = 23 mmHg, the EDV was 46 ml for cylindrical intramyocardial injections. At the same EDP, the EDV for spherical intramyocardial injections was 44 (made in mid-wall), 44 (made in endocardium) and 41 ml (made in epicardium) (Tab. 2).

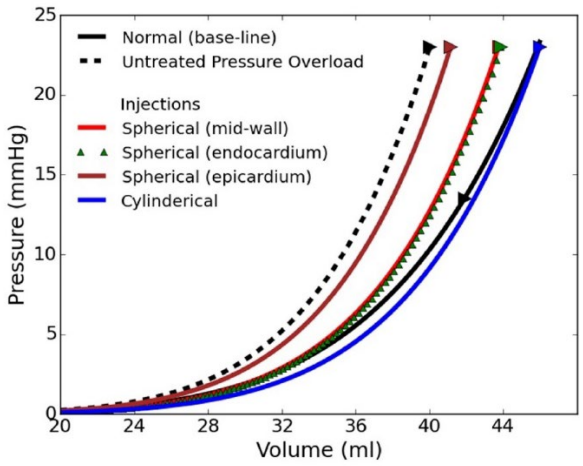

Figure 6: The intramyocardial injection treatment shifted EDPVR toward higher EDVs. The LV PV curve altered in the treated case such that it recovered toward the base-line case. The triangle represents EDV and EDP, and for the healthy condition, the curve has been extrapolated (pig #4)

The injected zones within the endocardial region experienced higher strains than in the untreated case (Fig. 7). Similarly to end systolic strains, end diastolic strains increased at the injection sites, as compared to the untreated case.

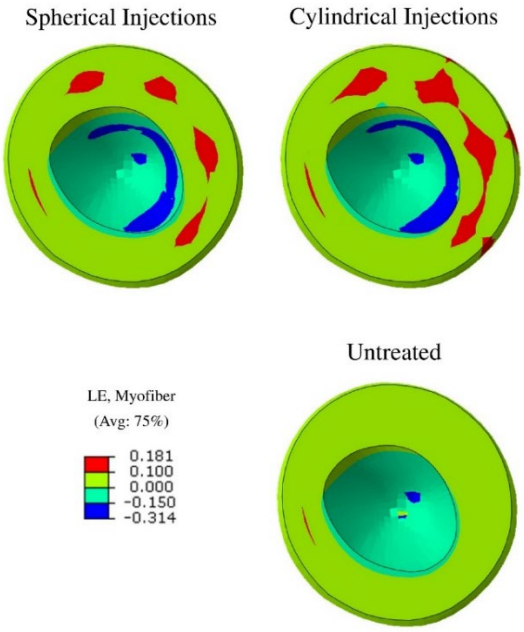

Figure 7: End-diastolic logarithmic strain distribution in the myofiber direction. The endocardial surface experienced high end-diastolic logarithmic myofiber strains at the injection sites. This is a top view, looking at the LV base

In all 4 subjects, the intramyocardial injection treatment was effective in increasing EDV (Figs. 6 and 8). Softening of LV (as seen in EDPVR) was observed for each subject. By adjusting injections number and the parameter $P_{scaling}$, the EDPVR was de-stiffened in such a way that EDPVR normalized toward normal EDPVR (Figs. 6 and 8).

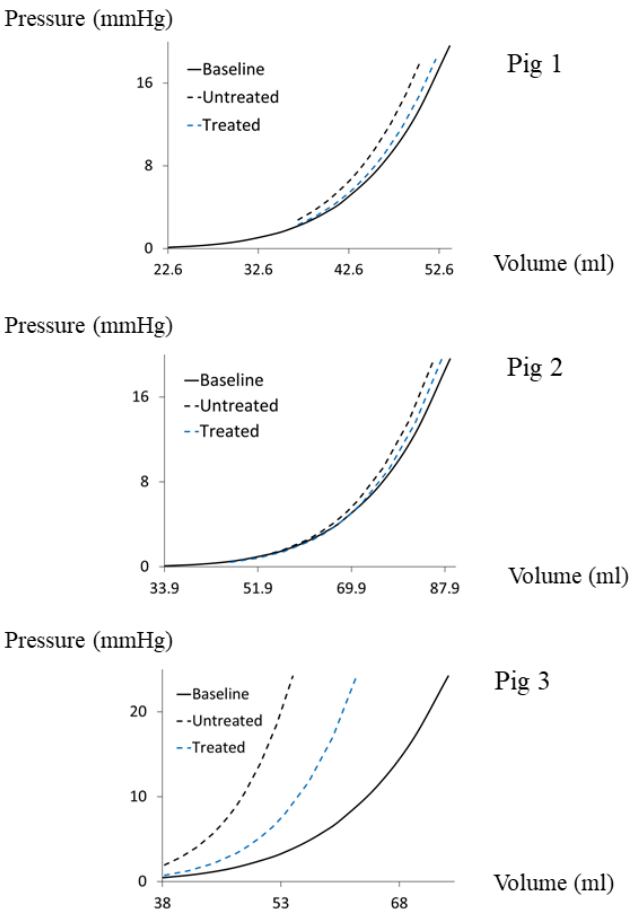

Figure 8: The intramyocardial injection treatment de-stiffened the LV in four pigs (also see Fig. 6). The curves correspond to: baseline (before overly stiff myocardium), untreated (after overly stiff myocardium and before injection treatment), and treated (after injection treatment). Subject-specific parameters affected the LV EDV after intramyocardial injection treatment. Subjects 1, 2 and 3 received 4, 4 and 16 injections, respectively; and for these subjects, parameter $P_{scaling}$ was 0.01, 0.3 and 1e-4, respectively

4 Discussion

To best of our knowledge, this is the first FE modeling study of a treatment for HPpEF that reduces the stiffness of the diastolic myocardium or extracellular matrix at strategic locations. These findings generate the hypothesis that regional intramyocardial injections of ALT-711 is an effective treatment for HFpEF. Although some of the findings are rather intuitive, the utility of the mathematical modeling is that we can assign specific numbers to the expected or predicted effects of this hypothesized novel treatment. For example, Tab. 2 and Fig. 5 show how EDV changes with different injection specifications. Specifically, with 8.0 ml of cylindrical intramyocardial injections in only the free wall and with EDP = 23 mmHg, EDV increased by 15.0% compared to the untreated case, and with 11 ml of cylindrical intramyocardial injections in both the free wall and the septum, EDV increased by 26.0%. These quantitative data could be used to identify the optimal parameters for ALT-711 intramyocardial injections.

Cylindrical intramyocardial injections that spread all the way from endocardium to epicardium were more effective in increasing EDV and improving the LV EDPVR (Tab. 2, Figs. 5 and 6). Moreover, the endocardium has a key role in intramyocardial injection treatment. Although the injection volume was less

for intramyocardial injections in the endocardium than in the mid-wall, they led to a higher increase in EDV (Tab. 2, Fig. 6). These computational results can lead to more directed and efficient animal-model experiments.

Although the free wall is more accessible for intramyocardial injections than the septum, the LV mechanics would be improved significantly if the intramyocardial injections were made in both the free wall and the septum (Fig. 5). We found that at EDP = 23 mmHg, with 8 ml intramyocardial injections only in the free wall, EDV increased by 15%, but that with 11 ml of intramyocardial injections in both the free wall and the septum, EDV increased by 26%, compared to the untreated case (Tab. 2).

The endocardial surface experienced high compressive strains in the injection regions, but we did not see noticeable distortions in injected regions, compared to the surrounding area (Figs. 4 and 7). The high compressive strains and regions with tensile strains may be a result of the alterations in mechanical properties caused by intramyocardial injections (inhomogeneous mechanical properties caused by injections). Although the intramyocardial injections did not lead to noticeable distortions in the injected sites, they noticeably altered the global mechanics of the LV, including EDV and EDPVR.

The injection-induced heterogenous strain distribution reveals an important factor in injection treatment. Regions with high or low strains may not function efficiently during systole in terms of contractile force generation. This potential effect of injections could be minimized using our FE models, and be implemented in experimental studies. This result shows the importance of FE modeling to optimize experimental studies.

An intrinsic part of the intramyocardial injection treatment presented here is the use of subject-specific data, an aspect of treatment that could make this solution more effective, given the subject to subject variability. The overly stiff EDPVR was normalized toward subject-specific healthy EDPVR by patient-oriented injections number and the parameter P_{scaling} (Fig. 8), a key finding because subject-specificity is not routinely considered in pharmacological strategies.

This study focused on modeling the effects of LV wall de-stiffening on the mechanics of LV, using intramyocardial injection treatment that targets abnormally stiff ECM. Although we used ALT-711 as the intramyocardial injection material because animal and human studies reported its safety and efficacy in de-stiffening LV when given systemically [1,20,21], percutaneous intramyocardial injections can be used with other softening agents (Tab. 4).

Table 4: Examples of agents that can be used in intramyocardial injections for de-stiffening

Agent/Publication	Species	Route of administration	Efficacy	Journal
Aminoguanidine [25]	dogs	oral	myocardial stiffness decreased	Diabetes
ALT-711[1,21]	dogs	oral	collagen upregulation reversed	PNAS
(proposed in this project)			myocardial stiffness decreased	Am. J. Physiol. Heart Circ. Physiol.
LCZ696 [2]	human	oral	NT-proBNP reduced	Lancet
Anakinra [28]	human	subcutaneous	systemic inflammatory reduced	Am. J. Cardio.
Saxagliptin/Tadalafil [30]	swine	oral	collagen deposition prevented	J. Am. Heart Assoc.

The focus of this study is on the theoretical foundation of the injection treatment prior to testing in animals and patients. We have used in silico models to understand mechanisms of HFpEF [9]. Therefore, the in silico model to examine the concept of injection treatment for stiff LV in HFpEF was created from and is supported by experimental data in the literature and from our lab. As noted above, de-stiffening therapy has been attempted in animals and patients but not intramyocardially. Given that this is novel, we believe it is prudent to test this approach in silico prior to *in vivo*. Along these lines, we have previously shown the translation of our computational models in a similar study where FE was used to model effects

of injections of a non-contractile material into myocardium for treatment of heart failure with reduced ejection fraction (HFrEF) [32]. That theoretical study led to pre-clinical [15] and clinical studies [23]. Our present computational model is more clinically relevant and is expected to guide relevant animal and pre-clinical studies.

5 Limitations and Future Directions

Heart failure is a complex phenomenon. There are many factors involved in onset and development of this disease. Our experimental data showed complex non-linear alterations in LV pressure and volume over time in HF. Interpretation of these alteration could provide valuable information about the development of HF, which is the subject of our on-going studies.

As any novel treatment, there may be side effects with our injection treatment approach for HFpEF. Of note, the systolic function of the heart such as stroke volume, end systolic volume and ejection fraction may be affected by injections. This paper was concerned with diastolic de-stiffening of LV by intramyocardial injections because diastolic overly stiff myocardium is at the core of HFpEF. As a future direction, effects of injection on other aspects of LV mechanics, including systolic behavior, still need to be assessed.

6 Conclusions

The results of FE modeling based on subject-specific data from 4 swine with LV pressure overload suggest that intramyocardial injection treatment can de-stiffen the EDPVR, and more importantly, the level of de-stiffening may be planned by adjusting intramyocardial injection specifications. Therefore, it may be possible to find a set of intramyocardial injections that result in the greatest increase in EDVs in the EDPVR, using our in silico subject-specific approach. There is likely an optimal level for EDPVR de-stiffening, after which LV function might not improve further, but defining that level will require actual implementation of intramyocardial injection treatment in animal experiments. This manuscript presents a hypothesis-generating novel approach of intramyocardial injection treatment for HFpEF; however, animal experiments are needed to verify these model predictions.

Acknowledgement: We thank Pamela Derish in the Department of Surgery, University of California San Francisco for assistance with proofreading the manuscript.

Funding: NIH grants R01-HL-077921, R01-HL-118627, 1R44HL135937 and U01-HL-119578.

Conflict of interest statement: The authors have no conflicts of interest to declare.

References

1. Asif M, Egan J, Vasan S, Jyothirmayi GN, Masurekar MR et al. An advanced glycation endproduct cross-link breaker can reverse age-related increases in myocardial stiffness. *Proceedings of the National Academy of Sciences* **2000**, 97(6): 2809-2813.
2. Avendano GF, Agarwal RK, Bashey RI, Lyons MM, Soni BJ et al. Effects of glucose intolerance on myocardial function and collagen-linked glycation. *Diabetes* **1999**, 48(7): 1443-1447.
3. Baillargeon B, Rebelo N, Fox D D, Taylor R L, Kuhl E et al. The living heart project: a robust and integrative simulator for human heart function. *European Journal of Mechanics-A/Solids* **2014**, 48: 38-47.
4. Benjamin EJ, Blaha MJ, Chiuve SE, Cushman M, Das S R et al. American heart association statistics committee and stroke statistics subcommittee. Heart disease and stroke statistics-2017 update: a report from the american heart association. *Circulation* **2017**, 135(10): 146-603.
5. Bhuiyan T, Maurer MS. Heart failure with preserved ejection fraction: persistent diagnosis, therapeutic enigma. *Current Cardiovascular Risk Reports* **2011**, 5(5): 440-449.
6. Biernacka A, Frangogiannis NG. Aging and cardiac fibrosis. *Aging and Disease* **2011**, 2(2): 158-173.

7. Bursi F, Weston SA, Redfield MM, Jacobsen SJ, Pakhomov S et al. Systolic and diastolic heart failure in the community. *JAMA* **2006**, 296(18): 2209.
8. Choy JS, Leng S, Acevedo-Bolton G, Shaul S, Fu L et al. Efficacy of intramyocardial injection of Algisyl-LVR for the treatment of ischemic heart failure in swine. *International Journal of Cardiology* **2018**, 255: 129-135.
9. Dabiri Y, Sack KL, Shaul S, Sengupta PP, Guccione JM. Relationship of transmural variations in myofiber contractility to left ventricular ejection fraction: implications for modeling heart failure phenotype with preserved ejection fraction. *Frontiers in Physiology* **2018**, 9: 1003.
10. Genet M, Lee LC, Nguyen R, Haraldsson H, Acevedo-Bolton G et al. Distribution of normal human left ventricular myofiber stress at end diastole and end systole: a target for in silico design of heart failure treatments. *Journal of Applied Physiology* **2014**, 117(2): 142-152.
11. Göktepe S, Acharya SNS, Wong J, Kuhl E. Computational modeling of passive myocardium. *International Journal for Numerical Methods in Biomedical Engineering* **2011**, 27(1): 1-12.
12. Guccione JM, McCulloch AD. Mechanics of active contraction in cardiac muscle: Part I-Constitutive relations for fiber stress that describe deactivation. *Journal of Biomechanical Engineering* **1993**, 115(1): 72-81.
13. Guccione JM, McCulloch AD, Waldman LK. Passive material properties of intact ventricular myocardium determined from a cylindrical model. *Journal of Biomechanical Engineering* **1991**, 113(1): 42-55.
14. Heidenreich PA, Albert NM, Allen LA, Bluemke DA, Butler J et al. American heart association advocacy coordinating committee; council on arteriosclerosis, thrombosis and vascular biology; council on cardiovascular radiology and intervention; council on clinical cardiology; council on epidemiology and prevention; stroke council. Forecasting the impact of heart failure in the united states: a policy statement from the american heart association. *Circulation: Heart Failure* **2013**, 6(3): 606-619.
15. Hiemstra JA, Lee DI, Chakir K, Gutiérrez-Aguilar M, Marshall KD et al. Saxagliptin and tadalafil differentially alter cyclic guanosine monophosphate (CGMP) signaling and left ventricular function in aortic-banded mini-swine. *Journal of the American Heart Association* **2016**, 5 (4): e003277.
16. Holzapfel GA, Ogden RW. Constitutive modelling of passive myocardium: a structurally based framework for material characterization. *Philosophical Transactions of the Royal Society A: Mathematical, Physical and Engineering Sciences* **2009**, 367(1902): 3445-3475.
17. Klotz S, Hay I, Dickstein ML, Yi GH, Wang J et al. Single-beat estimation of end-diastolic pressure-volume relationship: a novel method with potential for noninvasive application. American *Journal of Physiology-Heart and Circulatory Physiology* **2006**, 291(1): 403-412.
18. Lee LC, Wall ST, Klepach D, Ge L, Zhang Z et al. Algisyl-LVRTM with coronary artery bypass grafting reduces left ventricular wall stress and improves function in the failing human heart. *International Journal of Cardiology* **2013**, 168(3): 2022-2028.
19. Lee RJ, Hinson A, Bauernschmitt R, Matschke K, Fang Q et al. The feasibility and safety of Algisyl-LVRTM as a method of left ventricular augmentation in patients with dilated cardiomyopathy: Initial first in man clinical results. *International Journal of Cardiology* **2015**, 199: 18-24.
20. Little WC, Zile MR, Kitzman DW, Hundley WG, O'Brien TX et al. The effect of alagebrium chloride (ALT-711), a novel glucose cross-link breaker, in the treatment of elderly patients with diastolic heart failure. *Journal of Cardiac Failure* **2005**, 11(3): 191-195.
21. Liu J, Masurekar MR, Vatner DE, Jyothirmayi GN, Regan TJ et al. Glycation end-product cross-link breaker reduces collagen and improves cardiac function in aging diabetic heart. American *Journal of Physiology-Heart and Circulatory Physiology* **2003**, 285(6): 2587-2591.
22. Liu Y, Haddad T, Dwivedi G (2013). Heart failure with preserved ejection fraction. *Current Opinion in Cardiology* **2013**, 28(2): 187-196.
23. Mann DL, Lee RJ, Coats AJS, Neagoe G, Dragomir D et al. One-year follow-up results from AUGMENT-HF: a multicentre randomized controlled clinical trial of the efficacy of left ventricular augmentation with Algisyl in the treatment of heart failure. *European Journal of Heart Failure* **2016**, 18(3): 314-325.
24. Owan TE, Hodge D. O., Herges R. M., Jacobsen S. J., Roger V. L et al. Trends in prevalence and outcome of heart failure with preserved ejection fraction. *New England Journal of Medicine* **2006**, 355(3): 251-259.

25. Sabbah HN, Wang M, Gupta RC, Rastogi S, Ilsar I et al. Augmentation of left ventricular wall thickness with alginate hydrogel implants improves left ventricular function and prevents progressive remodeling in dogs with chronic heart failure. *JACC: Heart Failure* **2013**, 1(3): 252-258.
26. Sack KL, Aliotta E, Ennis DB, Choy JS, Kassab GS et al. Construction and validation of subject-specific biventricular finite-element models of healthy and failing swine hearts from high-resolution DT-MRI. *Frontiers in Physiology* **2018**, 9: 539.
27. Smit AJ, Hartog JWL, Voors AA, van Veldhuisen DJ. Advanced glycation endproducts in chronic heart failure. *Annals of the New York Academy of Sciences* **2008**, 1126(1): 225-230.
28. Solomon SD, Zile M, Pieske B, Voors A, Shah A et al. The angiotensin receptor neprilysin inhibitor LCZ696 in heart failure with preserved ejection fraction: a phase 2 double-blind randomised controlled trial. *The Lancet* **2012**, 380(9851): 1387-1395.
29. Streeter DD, Spotnitz HM, Patel DP, Ross J, Sonnenblick EH. Fiber orientation in the canine left ventricle during diastole and systole. *Circulation Research* **1969**, 24(3): 339-347.
30. Van Tassell BW, Arena R, Biondi-Zoccai G, McNair Canada J, Oddi C et al. Effects of interleukin-1 Blockade with anakinra on aerobic exercise capacity in patients with heart failure and preserved ejection fraction (from the D-HART Pilot Study). *American Journal of Cardiology* **2014**, 113(2): 321-327.
31. Vasan RS, Benjamin EJ, Levy D. Prevalence, clinical features and prognosis of diastolic heart failure: an epidemiologic perspective. *Journal of the American College of Cardiology* **1995**, 26(7): 1565-1574.
32. Wall ST, Walker JC, Healy KE, Ratcliffe MB, Guccione JM. Theoretical impact of the injection of material into the myocardium: a finite element model simulation. *Circulation* **2006**, 114(24): 2627-2635.
33. Wenk JF, Wall ST, Peterson RC, Helgerson SL, Sabbah HN et al. (2009): A method for automatically optimizing medical devices for treating heart failure: designing polymeric injection patterns. *Journal of Biomechanical Engineering* **2009**, 131(12): 121011.